



Article

# Ascorbic Acid, Ascorbate, and Dehydroascorbic Acid as Green Corrosion Inhibitors: A Computational Investigation

Bruno D. F. Souza <sup>1</sup>, Mateus R. Lage <sup>2</sup> , Adenilson Oliveira dos Santos <sup>2</sup> , Francisco Ferreira de Sousa <sup>3</sup> , Rodrigo Gester <sup>4</sup>, Stanislav R. Stoyanov <sup>5,\*</sup>  and Tarciso Andrade-Filho <sup>4,\*</sup> 

<sup>1</sup> Programa de Pós-Graduação em Química, Universidade Federal do Sul e Sudeste do Pará, Marabá 68505-080, PA, Brazil; bruno.souza@unifesspa.edu.br

<sup>2</sup> Universidade Federal do Maranhão—UFMA, R. Urbano Santos, Imperatriz 65900-410, MA, Brazil; mateus.lage@ufma.br (M.R.L.); adenilson.santos@ufma.br (A.O.d.S.)

<sup>3</sup> Instituto de Ciências Exatas e Naturais, Universidade Federal do Pará, Belém 66075-110, PA, Brazil; francisco\_ferreira@fisica.ufc.br

<sup>4</sup> Faculdade de Física, Universidade Federal do Sul e Sudeste do Pará, Marabá 68507-590, PA, Brazil; gester@unifesspa.edu.br

<sup>5</sup> Natural Resources Canada, CanmetENERGY Devon, 1 Oil Patch Drive, Devon, AB T9G 1A8, Canada

\* Correspondence: stanislav.stoyanov@nrncan-rncan.gc.ca (S.R.S.); tarcisofilho@unifesspa.edu.br (T.A.-F.)

**Abstract:** Ascorbic acid is widely used as an immunity-enhancing and antioxidant supplement for treating influenza and other virus-based illnesses. The lactone ring and the oxygenated groups make this system and derived structures attractive as possible environmentally friendly green corrosion inhibitors. Thus, we investigate the corrosion inhibition influence of ascorbic acid, ascorbate, and dehydroascorbic acid on the  $\alpha$ -Fe(110) surface using density functional theory calculations. The adsorption, density of states, and charge transfer results indicate that dehydroascorbic acid is this series's most potent corrosion inhibitor. The projected density of states near the Fermi energy reveals notable hybridization between the iron surface and dehydroascorbic acid adsorbed on it. The calculated structural, electronic, and energetic properties obtained in this work pave the way for understanding the corrosion inhibitory performance of the investigated systems.

**Keywords:** iron; green corrosion inhibitors; ascorbic acid; density functional theory calculations; tight binding formalism; charge density difference analysis



**Citation:** Souza, B.D.F.; Lage, M.R.; Santos, A.O.d.; Sousa, F.F.d.; Gester, R.; Stoyanov, S.R.; Andrade-Filho, T. Ascorbic Acid, Ascorbate, and Dehydroascorbic Acid as Green Corrosion Inhibitors: A Computational Investigation. *Corros. Mater. Degrad.* **2024**, *5*, 615–623. <https://doi.org/10.3390/cmd5040029>

Academic Editor: Angeliki G. Lekatou

Received: 16 September 2024  
Revised: 20 November 2024  
Accepted: 26 November 2024  
Published: 12 December 2024



**Copyright:** © 2024 by the authors. Licensee MDPI, Basel, Switzerland. This article is an open access article distributed under the terms and conditions of the Creative Commons Attribution (CC BY) license (<https://creativecommons.org/licenses/by/4.0/>).

## 1. Introduction

The antioxidant water-soluble vitamin L-ascorbic acid (AA) (Figure 1a) is naturally present in citrus and other fruits and thought to provide therapeutic advantages for people suffering from severe disorders [1]. AA has a dual role in the human body by absorbing iron and preventing dietary iron deficiency (anemia) [2,3]. AA is synthesized and accumulated in trees to protect against biotic and abiotic stress factors [4]. Consumption of ascorbic acid helps prevent various types of cancer due to its antioxidant activity, as it inhibits free radicals from causing damage to the human body [5].

The ascorbate anion (ASA) is identified as the deprotonated form of ascorbic acid (Figure 1). The antioxidant system of ascorbic acid, also known as ascorbate anion (ASA), is of significant importance [6]. The literature reveals that ascorbate, found at neutral pH, exhibits a more potent antioxidant action than that observed by the AA [7]. Ascorbic acid undergoes oxidation to yield another molecular form, dehydroascorbic acid (DHA). Both AA and ASA are recognized as electron donors, a property integral to their antioxidant process [8]. However, the electronic properties of DHA remain unexplored in the literature, though its potential as a neuroprotective drug in stroke treatment has been investigated [9].

In addition to all these properties, it is essential to highlight the use of AA in several studies as a corrosion inhibitor of metal systems [10]. Corrosion inhibition activity is associated with the adsorption of an inhibitor system and isolation of the metal surface

from the corrosive agent [11–13]. The adsorption of the green inhibitor molecules onto the metallic surface to be protected is strengthened by polar functional groups in the inhibitor [14,15]. Adsorption is a surface phenomenon that enhances corrosion protection by electrostatic interactions and charge transfer [16,17]. Li and colleagues have investigated the corrosion inhibition ability of AA on Q235 mild steel in acidic environments [18]. They observed that the corrosion inhibition was directly linked to the AA concentration. Ferreira et al. [19] have also investigated the corrosion inhibition of AA on mild steel using electrochemical and weight loss experimental techniques. They have found that DHA is an excellent mild steel corrosion inhibitor [19].

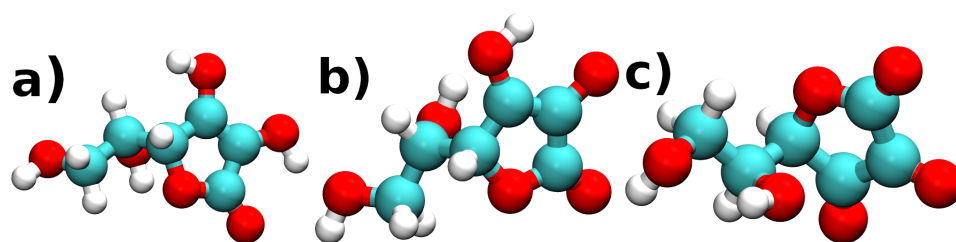


**Figure 1.** Molecular structures of (a) ascorbic acid, (b) ascorbate anion, and (c) dehydroascorbic acid. Carbon cyan; oxygen red; and hydrogen white.

Corrosion is a major industrial problem, as it continues to degrade infrastructure, causing huge annual financial losses, among other problems [20–23]. In one case study, inorganic inhibitors have been used over the years to avoid corrosion, although they are environmentally dangerous [24,25]. As a result, academia and industry professionals have focused on producing non-toxic, inexpensive, renewable, and efficient corrosion inhibitors [25–27]. The discovery of novel organic corrosion inhibitors, known as green corrosion inhibitors, has lately been recognized as critical, and have been explored over the years [10,28]. Green corrosion inhibitors typically contain polar functional groups and extended conjugated moieties that act as electron donors and adsorb chemically onto the metal surface [29]. When plant extracts are introduced to many industrial systems, they are thought to be rich in natural organic systems that reduce the corrosion rate through the adsorption of effective species on metal surfaces [17]. Compounds naturally present in plants, such as AA, are desirable as green eco-friendly inhibitors [30]. In this way, the conservation of the flora of the world's forests, notably the Amazon and boreal forests, is necessary so that new natural products can be identified and used for industrial applications. Besides improving the quality of life of the mostly indigenous peoples living in the forest, conservation adds value to the forest's natural products.

The self-consistent-charge density-functional tight-binding method (SCC-DFTB) method has been employed in several computational modeling investigations of eco-friendly protectors on metal surfaces [31–33]. Unlike isolated calculations or molecular dynamics, the SCC-DFTB enables the description of the molecule-surface interaction, taking into account bond formation, bond breakage, and charge transfer with accuracy close to that of Density Functional Theory (DFT) and a low computational cost. The adsorption and corrosion inhibition behavior of Schiff bases on iron was studied by Murmu et al. using DFTB. The preferred adsorption configuration of these inhibitors identified using DFTB is found to corroborate molecular simulations and experimental measurements [31]. Farhadian et al. explored the performance of a castor oil-based corrosion inhibitor for mild steel using both SCC-DFTB and DFT and experimental methods [32]. Recently, Santos et al. have employed SCC-DFTB to study the interactions of the biomolecules thymol and carvacrol with  $\alpha$ -Fe(110) [33].

Spinelli and coworkers [19] investigated the corrosion inhibition activity of AA and its oxidation products in pH = 2–6 solutions using electrochemical, microscopic, and weight loss techniques. Their study classified AA as a mixed-type inhibitor that acted simultaneously on anodic and cathodic reactions [19]. Considering that the enediol structure of ascorbic acid is conjugated to the carbonyl group on the lactone ring, this made the

resultant extended planar conjugated moiety containing two polar groups an effective adsorbate and theoretically a corrosion inhibitor system. In this work, we investigate computationally the behavior of AA as a corrosion inhibitor using the surface  $\alpha$ -Fe(110) by applying the SCC-DFTB method. The ASA and DHA are included in the study for comparison concerning the adsorption capacity of AA on the iron surface.

## 2. Computational Methods

The SCC-DFTB method [34], augmented by Grimme's third-order dispersion correction term [35], is applied in all calculations. For all potential pair interactions, the Trans3d Slater–Koster library is employed [36]. The calculations start by relaxing isolated systems, the investigated molecular structure, and the  $\alpha$ -Fe(110) surface. The Brillouin zone is sampled using the  $\Gamma$ -point only and a  $4 \times 4 \times 1$  mesh of k-points for the molecules and investigated surface, respectively. A slab of four monolayers is used to construct the  $(7 \times 7)$   $\alpha$ -Fe(110) surface in a vacuum region with a thickness of 10.0 Å. The  $\alpha$ -Fe(110) surface is selected as it is the most stable surface of iron commonly present under practical conditions [37]. During the adsorption process simulation, the slab's top two layers are relaxed, and the remaining layers are fixed.

After relaxing the molecular and crystalline structures in isolation, four adsorption configurations of each molecule are fully optimized on the  $\alpha$ -Fe(110) adsorbent surface. Calculating the adsorption energy yields the most stable configurations. Also, the charge density difference and density of states are obtained and analyzed in this work. The SCC-DFTB calculations are performed using the DFTB+ package release 24.1 [38]. The Mulliken charge analysis method is employed to estimate the charge transfer ( $\Delta Q(e)$ ) occurring to or from the  $\alpha$ -Fe(110) surface.

The adsorption energy  $E_{ads}$  is obtained as follows:

$$E_{ads} = E_{complex} - E_{surf} - E_{mol} \quad (1)$$

where  $E_{complex}$ ,  $E_{surf}$ , and  $E_{mol}$  describe the energy of the complex system,  $\alpha$ -Fe(001) surface, and inhibitor molecule at the adsorption configuration, respectively.

The charge density difference (CDD, denoted as  $\Delta\rho$ ) is calculated using the following equation:

$$\Delta\rho = \rho_{complex} - \rho_{surf} - \rho_{mol} \quad (2)$$

where  $\rho_{complex}$ ,  $\rho_{surf}$ , and  $\rho_{mol}$  stand for the charge density of the complex system,  $\alpha$ -Fe(001) surface, and inhibitor at the adsorption configuration. The optimized structures are visualized using the three-dimensional visualization programs VESTA [39] and VMD [40].

## 3. Results and Discussions

To gain a comprehensive understanding of the anticorrosive properties of each green inhibitor under investigation, we start our analysis by calculating the electronic HOMO-LUMO gap and the precise positions of their frontier orbitals [41]. The HOMO energies of the AA, ASA, and DHA inhibitors are determined to be  $-5.45$  eV,  $-1.81$  eV, and  $-5.75$  eV, respectively. The respective LUMO energies are  $-1.81$ ,  $0.16$  eV, and  $-4.23$  eV. Based on the frontier orbital energies, the HOMO-LUMO gap of these inhibitors is calculated as  $3.64$  eV,  $1.97$  eV, and  $1.52$  eV, respectively. According to the data obtained from this work, one can infer some points. The HOMO energy value of the ASA system is higher than the Fermi level of the surface investigated ( $-3.52$  eV). Considering the DHA inhibitor, the LUMO is below the Fermi level of the investigated surface. In the case of the AA inhibitor, its HOMO and LUMO frontier orbitals are below and slightly above the Fermi level of the  $\alpha$ -Fe(110) surface, respectively.

Considering the frontier orbital energy levels relative to the Fermi level of the studied surface in the context of the existing literature, it can be postulated that charge flows from the ASA to the surface, with the opposite process occurring for the DHA and AA corrosion

inhibitory systems [41]. Another point to be discussed is the energy gap between HOMO and LUMO energies. This parameter, as described in the literature, is of significant importance in understanding the reactivity of the green corrosion inhibitors on the investigated metal surface [41]. The smaller the HOMO-LUMO gap, the more reactive the inhibitor will be, and thus, the more significant the inhibition against corrosion. This understanding enlightens about the role of the HOMO-LUMO energy gap in the context of corrosion inhibition, and one appreciates its importance in this work [41]. The results obtained with molecular systems through the HOMO-LUMO gap indicate the following inhibition efficiency order: DHA > ASA > AA. This result corresponds with the findings described in the literature by Ferreira et al. [19]. The next step of the investigation focuses on producing detailed data to analyze how corrosion inhibitors interact with the investigated metal surface. It will help to understand the complex dynamics involved in the process and assess the effectiveness of the studied inhibitors against corrosion.

The iron lattice parameter, with a relaxed value of 2.90 Å, forms the basis of our study as we use it to create the  $\alpha$ -Fe(110) surface [33]. This value aligns with the one found in existing literature [42], reinforcing its validity. We start the interaction process after relaxing the molecular and crystalline structures in isolation. Four different initial adsorption configurations of the molecules relative to the iron surface—parallel via the furan ring (Figure S1a), and parallel via the dihydroxyethyl moiety (Figure S1c), perpendicular via the 3-hydroxyfuran group (or O-group in ASA or carbonyl in DHA) (Figure S1b), and perpendicular via the 2-hydroxyethyl group (Figure S1d)—are generated as starting points to model the interaction between adsorbent and adsorbate.

The fully optimized adsorbent-adsorbate structures formed by AA, ASA, and DHA and the  $\alpha$ -Fe(110) surface are shown in Figures 2–4, respectively. According to these figures, one can note that the molecules prefer to lay their rings parallel or almost parallel, deposited by a small angle on the surface of the adsorbent. This preferred adsorption configuration enlarges the contact area with the metallic surface [43].

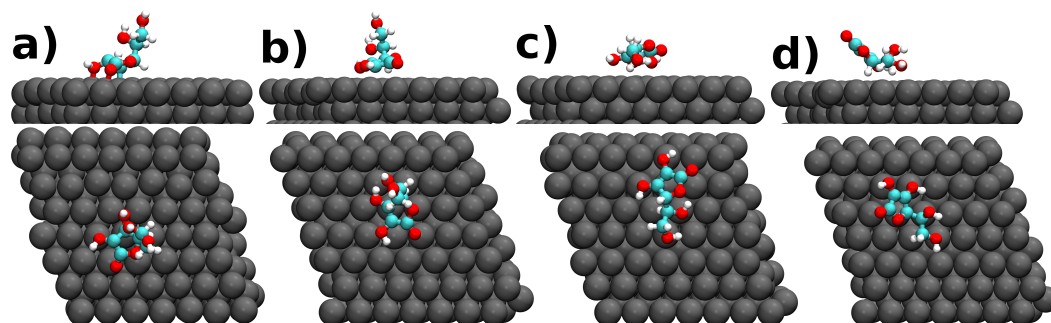


**Figure 2.** Relaxed adsorption geometries of AA on  $\alpha$ -Fe(110) surface shown along the  $c$  axis (top panel) and  $a$  axis (bottom panel). Color code: C cyan, H white, O red, Fe gray. Configurations (a–d) show the four computed ones with the highest level of energetic stability.

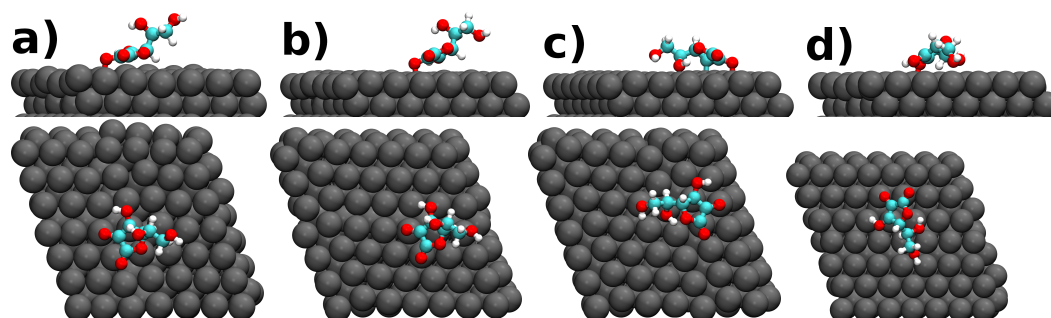


**Figure 3.** Relaxed adsorption geometries of ASA on  $\alpha$ -Fe(110) surface shown along the  $c$  axis (top panel) and  $a$  axis (bottom panel). Color code: C cyan, H white, O red, Fe gray. Configurations (a–d) show the four computed ones with the highest level of energetic stability.

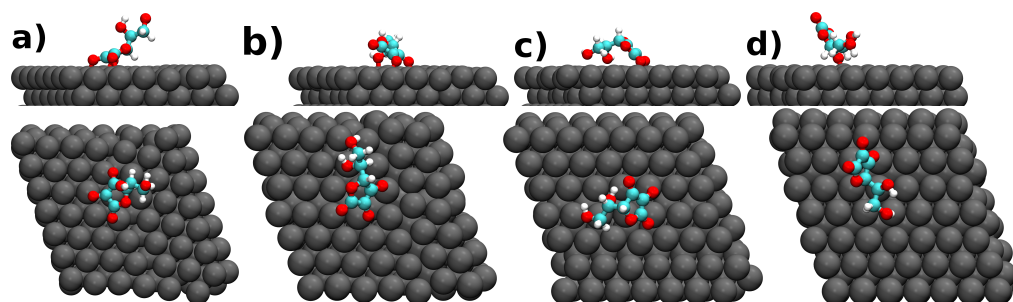


**Figure 4.** Relaxed adsorption geometries of DHA on  $\alpha$ -Fe(110) surface shown along the  $c$  axis (top panel) and  $a$  axis (bottom panel). Color code: C cyan, H white, O red, Fe gray. Configurations (a–d) show the four computed ones with the highest level of energetic stability.

In all 12 systems, the molecule-surface interactions are energetically favored over the isolated molecule and surface (Table 1). The greater the absolute value of adsorption energy, the stronger the contact between the inhibitor molecule and the investigated metal surface [44,45]. The adsorption energies show that DHA interacts more substantially with the  $\alpha$ -Fe(110) surface and is a better corrosion inhibitor than ASA and AA, in agreement with the experimental findings of Spinelli and coworkers [19]. It could be attributed to the more extended conjugation and planarity of DHA relative to ASA and AA. Our adsorption energy results compare favorably to SCC-DFTB data calculated for the sunflower oil-based corrosion inhibitors ( $E_{Ads} = 17.28$  eV) [46] and the castor oil-based corrosion inhibitors of 13.85 eV [32].

**Table 1.** Adsorption energy  $E_{Ads}$ , minimum distances  $h$ , and charge transfer  $\Delta Q$  from molecule to  $\alpha$ -Fe(110) surface at adsorption configurations (a–d) in Figures 2–4, S1 and S2. Positive  $\Delta Q$  values correspond to the donation of charge by the molecule.

Molecule@Fe(110)	$E_{Ads}$ (eV)	$h$ (Å)	$\Delta Q$ (e)
a) AA	−10.20	2.00	−0.47
b) AA	−6.47	2.23	0.20
c) AA	−5.25	2.28	0.30
d) AA	−3.25	2.28	0.20
a) ASA	−9.00	1.96	0.82
b) ASA	−7.63	1.92	0.77
c) ASA	−12.25	2.00	0.77
d) ASA	−12.80	1.87	0.92
a) DHA	−11.66	1.95	−0.40
b) DHA	−11.88	1.88	−0.34
c) DHA	−15.99	1.90	−0.46
d) DHA	−12.80	1.86	−0.33

The parallel adsorption configurations of AA and DHA are the most favorable (Table 1). The most favorable configuration for ASA is perpendicular via the 2-hydroxyethyl group, followed closely (0.55 eV) by the parallel via dihydroxyethyl. It has been reported elsewhere that systems in which the rings are parallel to the  $\alpha$ -Fe(110) give superior energy stabilization to those in which the molecules stay perpendicular to the surface [41,43,47–50]. Furthermore, it can be noted in Table 1 that the minimum interaction distances of the energetically most stable systems are shorter than the sum of the covalent radii pairs of Fe and C or Fe and O [51]. This result informs that the lactone ring is chemisorbed on the studied metallic surface [51]. It is known that the shorter the minimum distance formed between the molecular inhibitor and the investigated surface, the greater the adsorbent's adsorption activity [44].

It is essential to discuss the behavior of the three adsorbed molecules for the charge transfer, as considerable amounts of charge transfer are observed in all cases (Table 1). The ASA acts as a charge donor for Fe(110), while AA and DHA act as charge acceptors. In

less energetically stable adsorption configurations, such as (b–d) AA's charge-donating behavior, can also be noted. Since these less favorable AA adsorption configurations also involve considerable adsorption energy, it is believed that there is competition among the different configurations, and thus, AA can also act as a charge donor. The complex inhibition character of AA has been noted based on experimental studies [19].

The charge transfer can be observed using the charge density difference (CDD) to illustrate the charge transfer process from one system to another. Figure S2 shows the charge redistribution for the three investigated systems in their most stable adsorption states, i.e., (a) for AA, (b) for ASA, and (c) for DHA, as per Table 1. The yellow isosurface shows the electron accumulation, and the cyan isosurface shows the electron depletion areas. According to Figure S2, one can note charge transfer from the investigated surface towards AA and DHA molecules and the opposite process occurring for the ASA molecule system. It is worth mentioning that intense polarization of the studied surface is observed only with AA. One observes little polarization in the remaining two cases.

Calculating the projected density of states curves (PDOS) provides fundamental information on electronic properties involved in bonding interactions and charge transfer properties [51]. These results are shown in Figure 5a–c for the most stable adsorption configurations of AA, ASA, and DHA, respectively. A deeper look at these figures reveals that molecule-surface adsorption results in a substantial charge transfer and binding between the adsorbent and adsorbate because of unstructured density peaks near the Fermi energy, indicating hybridization between the systems involved [51]. The peak comes from the 2p orbitals of the investigated molecular carbon atoms. The similar behavior observed in the density of states for all systems is predicted because all molecules adsorb through analogous interaction forces on the studied surface.

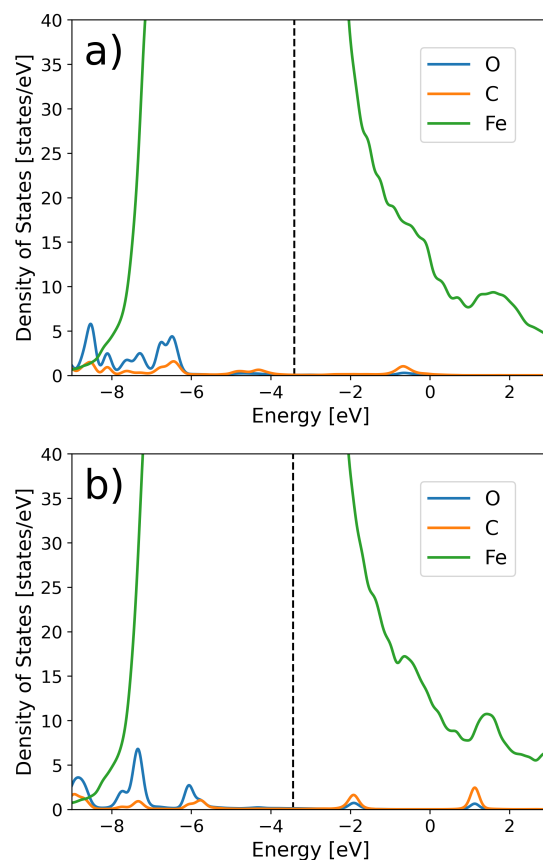
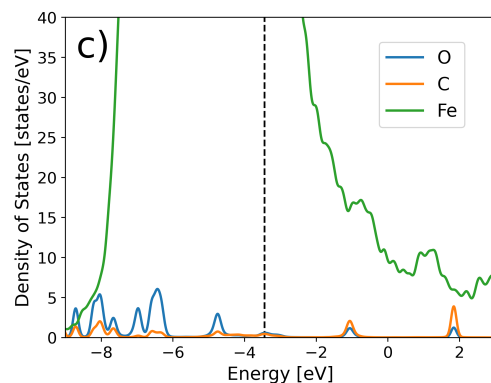


Figure 5. Cont.



**Figure 5.** Electronic projected density of states for (a) AA, (b) ASA, and (c) DHA adsorbed on  $\alpha$ -Fe(110) surface in their most stable adsorption configurations, according to Table 1. The vertical dashed line denotes the Fermi energy.

#### 4. Conclusions

A comprehensive theoretical study was conducted on the adsorption behavior of AA and derivative molecules used as corrosion inhibitors on the  $\alpha$ -Fe(110) surface. All the calculations were performed using the SCC-DFTB method. The study calculated the formed complexes' structural, energetic, and electronic properties. The results obtained in this work show that the adsorption strength of the investigated molecules is in the order of DHA > ASA > AA. Interaction distances, charge transfer, and density of states coupled with energetic properties make DHA the primary corrosion inhibitor among the investigated systems. In addition to corroborating the available experimental results, the computational investigations once again show an extensive capability to generate significant mechanistic insights into the interaction between metal surfaces and environmentally friendly green corrosion inhibitors.

**Supplementary Materials:** The following supporting information can be downloaded at: <https://www.mdpi.com/article/10.3390/cmd5040029/s1>, Figure S1: Initial AA adsorbed structures with perpendicular (figs. (b) and (d)) and parallel (figs. (a) and (c)) arrangements on a (110)  $\alpha$ -Fe(110) surface. The same configurations are used for systems containing ASA and DHA as adsorbates. Figure S2: Charge density difference maps of (a) AA, (b) ASA, and (c) DHA on  $\alpha$ -Fe(110) surface in their most stable adsorption configurations.

**Author Contributions:** Methodology, B.D.F.S.; Software, B.D.F.S.; Formal Analysis, B.D.F.S., M.R.L., A.O.d.S., F.F.d.S., R.G.; S.R.S. and T.A.-F.; Investigation, B.D.F.S., M.R.L., A.O.d.S., F.F.d.S., R.G., S.R.S. and T.A.-F.; Writing—Original Draft Preparation, B.D.F.S.; Writing—Review & Editing, B.D.F.S., M.R.L., A.O.d.S., F.F.d.S., R.G., S.R.S. and T.A.-F.; Visualization, B.D.F.S.; Supervision, S.R.S. and T.A.-F. All authors have read and agreed to the published version of the manuscript.

**Funding:** This research was funded by FAPESPA, CNPq and CAPES agencies and PERD and PDPG/CAPES programs.

**Institutional Review Board Statement:** Not applicable.

**Informed Consent Statement:** Not applicable.

**Data Availability Statement:** All data will be made available if requested.

**Acknowledgments:** The authors also thank the Digital Research Alliance of Canada (Alliance de recherche numérique du Canada) for the computational resources made available for this work. We wish to express our gratitude to Grammarly (<https://app.grammarly.com/>) for its valuable assistance in proofreading the initial draft of our manuscript, which significantly enhanced the language of this article. Following this tool, the authors reviewed and made necessary edits to the content, assuming full responsibility for the final publication.

**Conflicts of Interest:** The authors declare no conflicts of interest.

## References

1. Sulaiman, K.A.; Aljuhani, O.; Saleh, K.B.; Badreldin, H.A.; Harthi, A.A.; Alenazi, M.; Alharbi, A.; Algarni, R.; Harbi, S.A.; Alhammad, A.M.; et al. Ascorbic acid as an adjunctive therapy in critically ill patients with COVID-19: A propensity score matched study. *Sci. Rep.* **2021**, *11*, 17648.
2. Li, N.; Zhao, G.; Wu, W.; Zhang, M.; Liu, W.; Chen, Q.; Wang, X. The efficacy and safety of vitamin c for iron supplementation in adult patients with iron deficiency anemia. *JAMA Netw. Open* **2020**, *3*, e2023644. [[CrossRef](#)]
3. Piskin, E.; Cianciosi, D.; Gulec, S.; Tomas, M.; Capanoglu, E. Iron absorption: Factors, limitations, and improvement methods. *ACS Omega* **2022**, *7*, 20441. [[CrossRef](#)]
4. Bilska, K.; Wojciechowska, N.; Alipour, S.; Kalembe, E. Ascorbic acid—The little-known antioxidant in woody plants. *Antioxidants* **2019**, *8*, 645. [[CrossRef](#)]
5. Pawlowska, E.; Szczepanska, J.; Blasiak, J. Pro- and antioxidant effects of vitamin c in cancer in correspondence to its dietary and pharmacological concentrations. *Oxid. Med. Cell. Longev.* **2019**, *2019*, 1. [[CrossRef](#)]
6. Morais, M.A.; Fonseca, K.S.; Medeiros, R.A.; Andrada, L.V.P.; de Aquino Saraiva, R.; Ferreira-Silva, S.L.; Lima, A.L.; Simões, A. Use of the abrasion technique in minimal processing as an alternative to increase purchase acceptability and minimize browning in yam. *J. Sci. Food Agric.* **2021**, *102*, 121. [[CrossRef](#)] [[PubMed](#)]
7. Gramlich, G.; Zhang, J.; Nau, W.M. Increased Antioxidant Reactivity of Vitamin C at Low pH in Model Membranes. *J. Amer. Chem. Soc.* **2002**, *124*, 11252. [[CrossRef](#)]
8. Du, J.; Cullen, J.J.; Buettner, G.R. Ascorbic acid: Chemistry, biology and the treatment of cancer. *Biochim. Biophys. Acta Rev. Cancer* **2012**, *1826*, 443. [[CrossRef](#)]
9. Huang, J.; Agus, D.B.; Winfree, C.J.; Kiss, S.; Mack, W.J.; McTaggart, R.A.; Choudhri, T.F.; Kim, L.J.; Mocco, J.; Pinsky, D.J.; et al. Dehydroascorbic acid, a blood–brain barrier transportable form of vitamin c, mediates potent cerebroprotection in experimental stroke. *Proc. Natl. Acad. Sci. USA* **2001**, *98*, 11720. [[CrossRef](#)]
10. Sekine, I.; Nakahata, Y.; Tanabe, H. The corrosion inhibition of mild steel by ascorbic and folic acids. *Corros. Sci.* **1988**, *28*, 987. [[CrossRef](#)]
11. Jones, D. *Principles and Prevention of Corrosion*; MacMillan: New York, NY, USA, 1992.
12. Arthur, D.E.; Jonathan, A.; Ameh, P.O.; Anya, C. A review on the assessment of polymeric materials used as corrosion inhibitor of metals and alloys. *Int. J. Ind. Chem.* **2013**, *4*, 2. [[CrossRef](#)]
13. Guedes, D.; Martins, G.R.; Jaramillo, L.Y.A.; Dias, D.S.B.; da Silva, A.J.R.; Lutterbach, M.T.S.; Reznik, L.Y.; Sérvulo, E.F.C.; Alviano, C.S.; Alviano, D.S. Corrosion Inhibition of Mild Steel in Hydrochloric Acid Environments Containing Sonneratia caseolaris Leaf Extract. *ACS Omega* **2021**, *6*, 6893.
14. Fontana, M.; Staehle, K. *Advances in Corrosion Science and Technology*; Plenum Press: New York, NY, USA, 1970; Volume 1.
15. Stoyanova, A.; Petkova, G.; Peyerimhoff, S. Correlation between the molecular structure and the corrosion inhibiting effect of some pyrophthalone compounds. *Chem. Phys.* **2002**, *279*, 1. [[CrossRef](#)]
16. Damaskin, B.; Petrii, O.; Batrakov, V. *Adsorption*; Plenum Press: New York, NY, USA, 1971.
17. Shehata, O.S.; Korshed, L.A.; Attia, A. *Corrosion Inhibitors, Principles and Recent Applications*; InTech: London, UK, 2018.
18. Chidiebere, M.A.; Oguzie, E.E.; Liu, L.; Li, Y.; Wang, F. Ascorbic acid as corrosion inhibitor for Q235 mild steel in acidic environments. *J. Ind. Eng. Chem.* **2015**, *26*, 182. [[CrossRef](#)]
19. Ferreira, E.; Giacomelli, C.; Giacomelli, F.; Spinelli, A. Evaluation of the inhibitor effect of L-ascorbic acid on the corrosion of mild steel. *Mater. Chem. Phys.* **2004**, *83*, 129. [[CrossRef](#)]
20. Li, Y.; Xu, D.; Chen, C.; Li, X.; Jia, R.; Zhang, D.; Sand, W.; Wang, F.; Gu, T. Anaerobic microbiologically influenced corrosion mechanisms interpreted using bioenergetics and bioelectrochemistry: A review. *J. Mater. Sci. Technol.* **2018**, *34*, 1713. [[CrossRef](#)]
21. Goyal, M.; Kumar, S.; Bahadur, I.; Verma, C.; Ebenso, E.E. Organic corrosion inhibitors for industrial cleaning of ferrous and non-ferrous metals in acidic solutions: A review. *J. Mol. Liq.* **2018**, *256*, 565. [[CrossRef](#)]
22. Mhlanga, N.; Mphahlele, K. *Self-Standing Substrates*; Springer International Publishing: Berlin/Heidelberg, Germany, 2019; pp. 235–267.
23. Verma, C.; Hussain, C.M.; Ebenso, E.E. *Organic Corrosion Inhibitors: Synthesis, Characterization, Mechanism, and Applications*; Wiley: Hoboken, NJ, USA, 2021.
24. Wei, H.; Heidarshenas, B.; Zhou, L.; Hussain, G.; Li, Q.; Ostrikov, K.K. Green inhibitors for steel corrosion in acidic environment: state of art. *Mater. Today Sustain.* **2020**, *10*, 100044. [[CrossRef](#)]
25. Hossain, N.; Chowdhury, M.A.; Kchaou, M. An overview of green corrosion inhibitors for sustainable and environment friendly industrial development. *J. Adhes. Sci. Technol.* **2021**, *35*, 673. [[CrossRef](#)]
26. Sruthi, G.; Shakeela, K.; Shanmugam, R.; Rao, G.R. The corrosion inhibition of stainless steel by ferrocene–polyoxometalate hybrid molecular materials—Experimental and first principles studies. *Phys. Chem. Chem. Phys.* **2020**, *22*, 3329. [[CrossRef](#)]
27. Galvão, T.L.P.; Ferreira, I.; Kuznetsova, A.; Novell-Leruth, G.; Song, C.; Feiler, C.; Lamaka, S.V.; Rocha, C.; Maia, F.; Zheludkevich, M.L.; et al. CORDATA: An open data management web application to select corrosion inhibitors. *NPJ Mater. Degrad.* **2022**, *6*, 48. [[CrossRef](#)]
28. Zhang, Q.H.; Li, Y.Y.; Lei, Y.; Wang, X.; Liu, H.F.; Zhang, G.A. Comparison of the synergistic inhibition mechanism of two eco-friendly amino acids combined corrosion inhibitors for carbon steel pipelines in oil and gas production. *Appl. Surf. Sci.* **2022**, *583*, 152559. [[CrossRef](#)]

29. Shehata, O.S.; Khorshed, L.A.; Mandour, H.S. Effect of Acetamide Derivative and its Mn-Complex as Corrosion Inhibitor for Mild Steel in sulphuric Acid. *Egypt. J. Chem.* **2017**, *60*, 243.
30. Fazal, B.R.; Becker, T.; Kinsella, B.; Lepkova, K. A review of plant extracts as green corrosion inhibitors for CO<sub>2</sub> corrosion of carbon steel. *NPJ Mater. Degrad.* **2022**, *6*, 5. [[CrossRef](#)]
31. Murmu, M.; Saha, S.K.; Murmu, N.C.; Banerjee, P. Effect of stereochemical conformation into the corrosion inhibitive behaviour of double azomethine based Schiff bases on mild steel surface in 1 mol L<sup>-1</sup> HCl medium: An experimental, density functional theory and molecular dynamics simulation study. *Corr. Sci.* **2019**, *146*, 134. [[CrossRef](#)]
32. Farhadian, A.; Rahimi, A.; Safaei, N.; Shaabani, A.; Abdouss, M.; Alavi, A. A theoretical and experimental study of castor oil-based inhibitor for corrosion inhibition of mild steel in acidic medium at elevated temperatures. *Corr. Sci.* **2020**, *175*, 108871. [[CrossRef](#)]
33. Santos, R.S.; Barbosa, T.S.; Mafra, M.A.; Ribeiro, A.; Sousa, F.; Andrade-Filho, T. Simulation of Iron Corrosion Inhibition by Biological Molecules Thymol and Carvacrol. *Mater. Lett.* **2022**, *308*, 131249. [[CrossRef](#)]
34. Elstner, M.; Porezag, D.; Jungnickel, G.; Elsner, J.; Haugk, M.; Frauenheim, T.; Suhai, S.; Seifert, G. Self-consistent-charge density-functional tight-binding method for simulations of complex materials properties. *Phys. Rev. B* **1998**, *58*, 7260. [[CrossRef](#)]
35. Brandenburg, J.G.; Grimme, S. Accurate modeling of organic molecular crystals by dispersion-corrected density functional tight binding (DFTB). *J. Phys. Chem. Lett.* **2014**, *5*, 1785. [[CrossRef](#)]
36. Zheng, G.; Witek, H.A.; Bobadova-Parvanova, P.; Irle, S.; Musaev, D.G.; Prabhakar, R.; Morokuma, K.; Lundberg, M.; Elstner, M.; Köhler, C.; et al. Parameter Calibration of Transition-Metal Elements for the Spin-Polarized Self-Consistent-Charge Density-Functional Tight-Binding (DFTB) Method: Sc, Ti, Fe, Co, and Ni. *J. Chem. Theory Comput.* **2007**, *3*, 1349. [[CrossRef](#)]
37. Hu, J.; Wang, C.; He, S.; Zhu, J.; Wei, L.; Zheng, S. A DFT-Based Model on the Adsorption Behavior of H<sub>2</sub>O, H<sup>+</sup>, Cl<sup>-</sup>, and OH<sup>-</sup> on Clean and Cr-Doped Fe(110) Planes. *Coatings* **2018**, *8*, 51. [[CrossRef](#)]
38. Hourahine, B.; Aradi, B.; Blum, V.; Bonafé, F.; Buccheri, A.; Camacho, C.; Cevallos, C.; Deshayé, M.Y.; Dumitrică, T.; Dominguez, A.; et al. DFTB+, a software package for efficient approximate density functional theory based atomistic simulations. *J. Chem. Phys.* **2020**, *152*, 124101. [[CrossRef](#)] [[PubMed](#)]
39. Momma, K.; Izumi, F. VESTA 3 for three-dimensional visualization of crystal, volumetric and morphology data. *J. Appl. Crystallogr.* **2011**, *44*, 1272. [[CrossRef](#)]
40. Humphrey, W.; Dalke, A.; Schulten, K. VMD: Visual molecular dynamics. *J. Mol. Graph.* **1996**, *14*, 33. [[CrossRef](#)]
41. Guo, L.; Qi, C.; Zheng, X.; Zhang, R.; Shen, X.; Kaya, S. Toward understanding the adsorption mechanism of large size organic corrosion inhibitors on an Fe(110) surface using the DFTB method. *RSC Adv.* **2017**, *7*, 29042. [[CrossRef](#)]
42. Zemmann, J. Crystal structures, 2nd edition. Vol. 1 by R. W. G. Wyckoff. *Acta Crystallogr.* **1965**, *18*, 139. [[CrossRef](#)]
43. Singh, A.; Ansari, K.R.; Quraishi, M.A.; Lin, Y. *Corrosion Inhibitors*; IntechOpen: London, UK, 2019.
44. Tian, G.; Yuan, K. Performance and Mechanism of Alkylimidazolium Ionic Liquids as Corrosion Inhibitors for Copper in Sulfuric Acid Solution. *Molecules* **2021**, *26*, 4910. [[CrossRef](#)]
45. Abdallah, M.; Soliman, K.A.; Jahdaly, B.A.A.; Al-Fahemi, J.H.; Hawsawi, H.; Altass, H.M.; Motawea, M.S.; Al-Juaid, S.S. Natural parsley oil as a green and safe inhibitor for corrosion of X80 carbon steel in 0.5 M H<sub>2</sub>SO<sub>4</sub> solution: A chemical, electrochemical, DFT and MC simulation approach. *RSC Adv.* **2022**, *12*, 2959. [[CrossRef](#)]
46. Farhadian, A.; Rahimi, A.; Safaei, N.; Shaabani, A.; Sadeh, E.; Abdouss, M.; Alavi, A. Exploration of Sunflower Oil As a Renewable Biomass Source to Develop Scalable and Highly Effective Corrosion Inhibitors in a 15% HCl Medium at High Temperatures. *ACS Appl. Mater. Interf.* **2021**, *13*, 3119. [[CrossRef](#)]
47. Zarrouk, A.; Zarrok, H.; Salghi, R.; Hammoutil, B.; Al-Deyab, S.; Touzanil, R. Bouachrine, M.; Warad, I.; Hadda, T.B. A Theoretical Investigation on the Corrosion Inhibition of Copper by Quinoxaline Derivatives in Nitric Acid Solution. *Int. J. Electrochem. Sci.* **2012**, *7*, 6353. [[CrossRef](#)]
48. Fang, J.; Li, J. Quantum chemistry study on the relationship between molecular structure and corrosion inhibition efficiency of amides. *J. Mol. Struct. THEOCHEM* **2002**, *593*, 179. [[CrossRef](#)]
49. Zhu, J.; Chen, S. A Theoretical Investigation on the Inhibition Efficiencies of Some Schiff bases as Corrosion Inhibitors of Steel in Hydrochloric Acid. *Int. J. Electrochem. Sci.* **2012**, *7*, 11884. [[CrossRef](#)]
50. Kumar, D.; Jain, V.; Rai, B. Imidazole derivatives as corrosion inhibitors for copper: A DFT and reactive force field study. *Corr. Sci.* **2018**, *142*, 102. [[CrossRef](#)]
51. Lgaz, H.; Lee, H.S. Facile preparation of new hydrazone compounds and their application for long-term corrosion inhibition of N80 steel in 15% HCl: An experimental study combined with DFTB calculations. *J. Mol. Liq.* **2022**, *347*, 117952. [[CrossRef](#)]

**Disclaimer/Publisher's Note:** The statements, opinions and data contained in all publications are solely those of the individual author(s) and contributor(s) and not of MDPI and/or the editor(s). MDPI and/or the editor(s) disclaim responsibility for any injury to people or property resulting from any ideas, methods, instructions or products referred to in the content.